

Engineering Notes

ENGINEERING NOTES are short manuscripts describing new developments or important results of a preliminary nature. These Notes should not exceed 2500 words (where a figure or table counts as 200 words). Following informal review by the Editors, they may be published within a few months of the date of receipt. Style requirements are the same as for regular contributions (see inside back cover).

Lateral-Directional Aircraft Dynamics Under Static Moment Nonlinearity

Tiauw Hiong Go*

Nanyang Technological University,
Singapore 639798, Republic of Singapore

DOI: 10.2514/1.39025

I. Introduction

THIS Note specifically focuses on the aircraft lateral-directional dynamics in the presence of nonlinearity in lateral moments with respect to sideslip (static lateral moments). Such nonlinearity is often encountered during flight in the regimes in which the aerodynamic properties are nonlinear: for example, during high-angle-of-attack flight. In the previous works by the author [1–3], which focus on the multiple-degree-of-freedom wing-rock dynamics at high angles of attack, the results imply that by itself, the nonlinearity in the static lateral moments [such as that considered here (cubic polynomial with respect to sideslip)] does not lead to wing rock. Those analyses, however, consider only the situation in which the nonlinearity is relatively weak. In [4], cubic nonlinearity of static lateral moments with respect to sideslip is shown to cause wing rock in a multimode system in certain conditions. Because of these seemingly discrepant findings, the topic is revisited here.

This Note presents detailed analysis of the lateral-directional motion when the cubic type of static lateral moment nonlinearity is present in the system. The equations of motion as derived in [3] are used as the basis for the analysis. To gain physical insight into the problem, an analytical approach using the multiple-time-scales (MTS) method is used (see, for example, [5,6]). Both weak and strong nonlinearity cases are considered.

II. Equations of Motion

Figure 1 shows an example of nonlinear variations in rolling and yawing moment coefficients C_l and C_n with respect to the sideslip angle β . The variations shown in the figure are typical for fighter aircraft at high angles of attack, although the strength of the variations may vary with configurations and flight conditions. Such nonlinearity can be represented by adding cubic β terms in the expression for the lateral moments. All other nonlinearities are neglected in the current analysis, and thus the lateral moments can be expressed as follows:

$$\begin{aligned} L/I_{xx} &= L_\beta \beta + L_{\beta_1} \beta^3 + L_p p + L_r r + L_{\dot{\beta}} \dot{\beta} \\ N/I_{zz} &= N_\beta \beta + N_{\beta_1} \beta^3 + N_p p + N_r r + N_{\dot{\beta}} \dot{\beta} \end{aligned} \quad (1)$$

where p is roll rate; r is yaw rate; β is sideslip angle; $\dot{\beta}$ is sideslip rate; I_{xx} and I_{zz} are the moments of inertia of the aircraft about its body x and z axes, respectively; L and N are the total rolling and yawing moments, respectively; L_i and N_i , where $i = \beta, p, r$, and $\dot{\beta}$ are the usual linear stability derivatives; and L_{β_1} and N_{β_1} are the coefficients of the cubic sideslip terms, which represent the nonlinearity. In this formulation, the coupling between the longitudinal and the lateral-directional modes is neglected and the lateral-directional modes are analyzed separately.

In [3], the nonlinear equations describing the attitude dynamics of a rigid aircraft with a conventional configuration with three rotational degrees of freedom have been derived. In the derivation, the trajectory of the center of mass of the aircraft is assumed to be straight and horizontal and is not affected by its attitude motion. The lateral-directional part of the equations are used as the basis of the analysis here and will not be rederived. With the preceding simplifying assumption on the nonlinearity, the equations of motion can be written as follows:

$$\begin{aligned} \ddot{\beta} + \omega_1^2 \beta &= \tilde{\eta}_1 \dot{\beta} + \tilde{\kappa}_2 \phi + \tilde{\eta}_2 \dot{\phi} + \tilde{\lambda} \beta^3 \\ \ddot{\phi} &= \tilde{\kappa}_1 \beta + \tilde{\kappa}_3 \phi + \tilde{\xi}_1 \dot{\phi} + \tilde{\xi}_2 \dot{\beta} + \tilde{\sigma} \beta^3 \end{aligned} \quad (2)$$

where ϕ is the roll angle and

$$\begin{aligned} \omega_1^2 &= -1/(1 - n_1 n_3) [(L_\beta + n_1 N_\beta) s\alpha - (N_\beta + n_3 L_\beta) c\alpha] \\ \tilde{\eta}_1 &= 1/(1 - n_1 n_3) [n_3 L_r + N_r - (L_r + n_1 N_r) t\alpha \\ &\quad + (L_{\dot{\beta}} + n_1 N_{\dot{\beta}}) s\alpha - (n_3 L_{\dot{\beta}} + N_{\dot{\beta}}) c\alpha] \\ \tilde{\kappa}_2 &= (g/V) c\alpha / (1 - n_1 n_3) [- (N_r + n_3 L_r) + (L_r + n_1 N_r) t\alpha] \\ \tilde{\eta}_2 &= (g/V) c\alpha + 1/(1 - n_1 n_3) [(L_p + L_r t\alpha + n_1 (N_p + N_r t\alpha)) s\alpha \\ &\quad - (N_p + N_r t\alpha + n_3 (L_p + L_r t\alpha)) c\alpha] \\ \tilde{\lambda} &= 1/(1 - n_1 n_3) [(L_{\beta_1} + n_1 N_{\beta_1}) s\alpha - (n_3 L_{\beta_1} + N_{\beta_1}) c\alpha] \\ \tilde{\kappa}_1 &= 1/(1 - n_1 n_3) (L_\beta + n_1 N_\beta) \\ \tilde{\kappa}_3 &= (g/V) (L_r + n_1 N_r) / (1 - n_1 n_3) \\ \tilde{\xi}_1 &= 1/(1 - n_1 n_3) (L_p + n_1 N_p + (L_r + n_1 N_r) t\alpha) \\ \tilde{\xi}_2 &= 1/(1 - n_1 n_3) (L_{\dot{\beta}} + n_1 N_{\dot{\beta}} - (L_r + n_1 N_r) / c\alpha) \\ \tilde{\sigma} &= 1/(1 - n_1 n_3) (L_{\beta_1} + n_1 N_{\beta_1}) \end{aligned} \quad (3)$$

where g is the gravitational acceleration; V is the nominal airspeed; n_1 and n_3 are defined as I_{xz}/I_{xx} and I_{xz}/I_{zz} , respectively; and $c\alpha$, $s\alpha$, and $t\alpha$ denote $\cos \alpha_0$, $\sin \alpha_0$, and $\tan \alpha_0$, respectively, where α_0 is the nominal angle of attack of the flight. Note that the coefficients of the nonlinear lateral moment terms L_{β_1} and N_{β_1} appear only in $\tilde{\lambda}$ and $\tilde{\sigma}$.

III. Weak Nonlinearity Case

As in [3], Eq. (2) is parameterized by imposing several assumptions. First, only the case in which the damping terms are

Received 10 June 2008; revision received 20 August 2008; accepted for publication 25 August 2008. Copyright © 2008 by Tiauw Hiong Go. Published by the American Institute of Aeronautics and Astronautics, Inc., with permission. Copies of this paper may be made for personal or internal use, on condition that the copier pay the \$10.00 per-copy fee to the Copyright Clearance Center, Inc., 222 Rosewood Drive, Danvers, MA 01923; include the code 0731-5090/09 \$10.00 in correspondence with the CCC.

*Assistant Professor, School of Mechanical and Aerospace Engineering, 50 Nanyang Avenue. Senior Member AIAA.

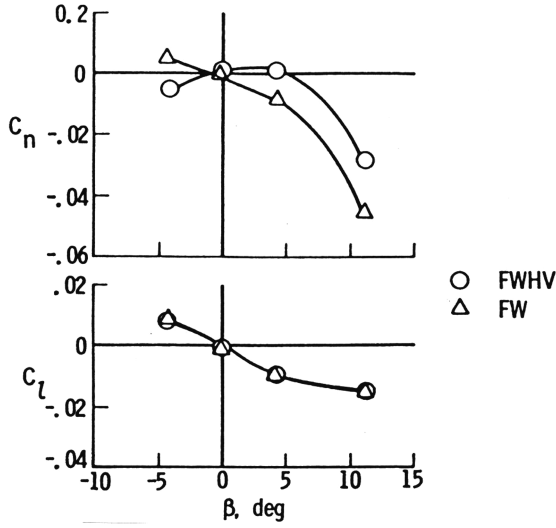


Fig. 1 Variation of lateral moment coefficients with sideslip for full-configuration aircraft (FWHV) and for the fuselage-wing combination only (FW) [10].

small is considered. Second, it is assumed that $g/(\omega_1 V)$ is small, where ω_1 represents the dominant frequency of the rotational motion. This assumption indicates that the ratio of the time scale of the translational motion to that of the rotational motion is small, which implies that the rotational motion is uncoupled with the translational motion. Additionally, in this section, the weak nonlinearity case is considered, which can be mathematically expressed as

$$\lim_{\mathbf{x} \rightarrow 0} \frac{|N(\mathbf{x})|}{|\mathbf{x}|} \rightarrow 0 \quad (4)$$

where $\mathbf{x} = \{\beta \ \phi \ \dot{\beta} \ \dot{\phi}\}^T$ and $N(\mathbf{x})$ represents the nonlinear terms in the equation. With these assumptions, the lateral-directional equations of motion of the aircraft become

$$\begin{aligned} \ddot{\beta} + \omega_1^2 \beta &= \epsilon[\eta_1 \dot{\beta} + \kappa_2 \phi + \eta_2 \dot{\phi} + \lambda \beta^3] \\ \ddot{\phi} &= \kappa_1 \beta + \epsilon[\kappa_3 \phi + \xi_1 \dot{\phi} + \xi_2 \dot{\beta} + \sigma \beta^3] \end{aligned} \quad (5)$$

where $0 < \epsilon \ll 1$. In the preceding equation, $\tilde{(\cdot)} \equiv \epsilon(\cdot)$, except for $\tilde{\kappa}_1 \equiv \kappa_1$.

Applying the MTS method to Eq. (5) as detailed in [3] with

$$t \rightarrow \{\tau_0, \tau_1, \tau_2\} \quad \tau_0 = t \quad \tau_1 = \epsilon t \quad \tau_2 = \epsilon^2 t \quad (6)$$

leads to approximate solutions of the following form (these results are subsumed in those obtained in [3] and thus the details are not repeated here):

$$\begin{aligned} \beta_0 &= A_1(\tau_2) \sin \Psi_1 \quad \Psi_1 \equiv \omega_1 \tau_0 + B_1(\tau_2) \\ \phi_0 &= -\frac{\kappa_1}{\omega_1^2} A_1(\tau_2) \sin \Psi_1 + A_2(\tau_2) \sin[\omega_2 \tau_1 + B_2(\tau_2)] \end{aligned} \quad (7)$$

where $\omega_2^2 = -(\kappa_3 + \kappa_1 \kappa_2 / \omega_1^2)$. The slowly varying amplitudes A_1 and A_2 and phase corrections B_1 and B_2 in Eq. (7) are governed by

$$\frac{dA_1}{d\tau_2} = \frac{\mu}{2} A_1 \quad \frac{dB_1}{d\tau_2} = r A_1^2 \quad \frac{dA_2}{d\tau_2} = \frac{\vartheta}{2} A_2 \quad \frac{dB_2}{d\tau_2} = 0 \quad (8)$$

where

$$\mu = \eta_1 - \frac{\kappa_1}{\omega_1^2} \eta_2 \quad r = -\frac{\kappa_1 \kappa_2}{2\omega_1^3} \quad \vartheta = -\left(\xi_2 + \frac{\kappa_1 \eta_2}{\omega_1^2}\right) \quad (9)$$

In this case, A_1 diverges when $\mu > 0$ and decays to zero when $\mu < 0$. Similarly, A_2 diverges when $\vartheta > 0$ and decays to zero when $\vartheta < 0$. Thus, the condition for asymptotically stable motion is $\mu < 0$ and $\vartheta < 0$. This analysis also indicates that the weak L_{β_1} and N_{β_1}

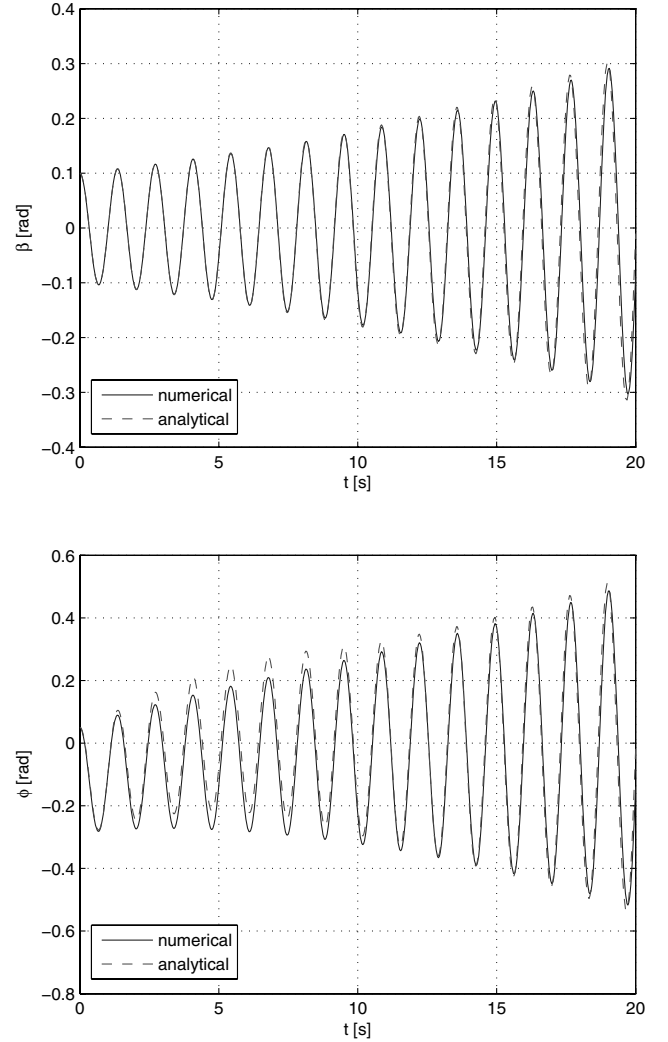


Fig. 2 Responses β and ϕ for $C_{l\beta_1} = 0.1$ and $C_{n\beta_1} = 0.04$ with initial conditions $(\beta_0, \phi_0) = (0.1, 0.05)$ rad.

nonlinearities do not give rise to a limit-cycle type of motion (wing rock), which confirms the results in [3].

Using the parameters of a generic fighter aircraft as given in the Appendix, the lateral-directional dynamic responses of the system are simulated. Figure 2 shows such responses for the initial conditions of $\beta(0) = 0.1$ rad and $\phi(0) = 0.05$ rad. In this case, $\mu > 0$ and $\vartheta < 0$, and as predicted by the analysis, the β and ϕ responses exhibit oscillations with increasing amplitudes (unstable). The amplitude asymmetry in the ϕ response relative to $\phi = 0$ during the transient (the first 10 s) is due to the stable homogeneous mode that appears in the ϕ solution, as indicated in Eq. (7). Both analytical and numerical integration results are plotted in Fig. 2. As can be seen from the figure, the analytical approximation obtained by the MTS method is fairly accurate in predicting both the amplitude and frequency of the responses. Various simulations performed also indicate that the analytical results are accurate in predicting the stability of the system.

IV. Strong Nonlinearity Case

An interesting case arises when the nonlinearity due to L_{β_1} and N_{β_1} becomes stronger. In this case, the terms $\lambda \beta^3$ and $\sigma \beta^3$ in Eq. (5) can no longer be put in the $\mathcal{O}(\epsilon)$ group. The mathematical formulation of the problem becomes as follows:

$$\begin{aligned} \ddot{\beta} + \omega_1^2 \beta &= \lambda \beta^3 + \epsilon[\eta_1 \dot{\beta} + \kappa_2 \phi + \eta_2 \dot{\phi}] \\ \ddot{\phi} &= \kappa_1 \beta + \sigma \beta^3 + \epsilon[\kappa_3 \phi + \xi_1 \dot{\phi} + \xi_2 \dot{\beta}] \end{aligned} \quad (10)$$

The MTS method with three time-scale extensions as in Eq. (6) are invoked to the problem. By these extensions, Eqs. (10) become partial-differential equations as follows:

$$\begin{aligned} \frac{\partial^2 \beta}{\partial \tau_0^2} + \omega_1^2 \beta + \epsilon^3 \left(2 \frac{\partial^2 \beta}{\partial \tau_0 \partial \tau_1} \right) + \epsilon \left(2 \frac{\partial^2 \beta}{\partial \tau_0 \partial \tau_2} + \frac{\partial^2 \beta}{\partial \tau_1^2} \right) \\ + \epsilon^3 \left(2 \frac{\partial^2 \beta}{\partial \tau_1 \partial \tau_2} \right) + \dots = \lambda \beta^3 + \epsilon \left(\eta_1 \frac{\partial \beta}{\partial \tau_0} + \kappa_2 \phi + \eta_2 \frac{\partial \phi}{\partial \tau_0} \right) \\ + \epsilon^3 \left(\eta_1 \frac{\partial \beta}{\partial \tau_1} + \eta_2 \frac{\partial \phi}{\partial \tau_1} \right) + \dots \\ \frac{\partial^2 \phi}{\partial \tau_0^2} + \epsilon^3 \left(2 \frac{\partial^2 \phi}{\partial \tau_0 \partial \tau_1} \right) + \epsilon \left(2 \frac{\partial^2 \phi}{\partial \tau_0 \partial \tau_2} + \frac{\partial^2 \phi}{\partial \tau_1^2} \right) + \epsilon^3 \left(2 \frac{\partial^2 \phi}{\partial \tau_1 \partial \tau_2} \right) \\ + \dots = \kappa_1 \beta + \sigma \beta^3 + \epsilon \left(\kappa_3 \phi + \xi_1 \frac{\partial \phi}{\partial \tau_0} + \xi_2 \frac{\partial \beta}{\partial \tau_0} \right) \\ + \epsilon^3 \left(\xi_1 \frac{\partial \phi}{\partial \tau_1} + \xi_2 \frac{\partial \beta}{\partial \tau_1} \right) + \dots \end{aligned} \quad (11)$$

Order-by-order analysis is then performed on the preceding equation. The leading-order β equation is

$$\mathcal{O}(1): \frac{\partial^2 \beta}{\partial \tau_0^2} + \omega_1^2 \beta = \lambda \beta^3 \quad (12)$$

Equation (12) is the partial-differential equation version of the undamped Duffing equation, which is known to have a periodic solution. Because Eq. (12) is a partial-differential equation, the constants of the integration are allowed to vary with the other independent variables, which are the slower time scales τ_1 and τ_2 . By using the fact that at the amplitude of oscillation, $\partial \beta / \partial \tau_0 = 0$, and by multiplying Eq. (12) with $\partial \beta / \partial \tau_0$ and then integrating, the following equation is obtained:

$$\left(\frac{\partial \beta}{\partial \tau_0} \right)^2 = \frac{\lambda}{2} (A_1^2(\tau_1, \tau_2) - \beta^2) \left(\frac{2\omega_1^2}{\lambda} - A_1^2(\tau_1, \tau_2) - \beta^2 \right) \quad (13)$$

where $A_1(\tau_1, \tau_2)$ is the slowly varying amplitude of the motion. Separating the variables and then integrating leads to the following solution [7]:

$$\beta = A_1 \operatorname{sn} \left(\omega_1 \sqrt{1 - \frac{\lambda}{2\omega_1^2} A_1^2} \tau_0 \right) \quad (14)$$

where sn is the Jacobian elliptic function. Equation (14) shows that β is oscillatory, and for small-amplitude motions, it can be approximated fairly well by [7,8]

$$\beta(\tau_0, \tau_1, \tau_2) = A_1(\tau_1, \tau_2) \sin \Theta_1 \quad \Theta_1 \equiv \bar{\omega}_1 \tau_0 + B_1(\tau_1, \tau_2) \quad (15)$$

where $B_1(\tau_1, \tau_2)$ represents the phase correction of the solution and

$$\bar{\omega}_1 \approx \omega_1 \left(1 - \frac{3\lambda}{8\omega_1^2} A_1^2 \right)$$

This representation simplifies the analysis further by the elimination of the mathematical operations involving nonelementary functions.

Equation (15) indicates that the frequency of the solution is dependent upon its amplitude. This is a consequence of approximating a nonelementary solution in terms of elementary functions. The dependence of the frequency on the amplitudes complicates the analysis of the higher-order terms. However, for small-amplitude motions ($A_1 \ll 1$), the variation of $\bar{\omega}_1$ due to A_1 can be neglected. Hence, $\bar{\omega}$ will be assumed constant in the subsequent analysis.

Substituting Eq. (15) into the leading-order terms of the ϕ equation from Eq. (11) and then integrating twice with respect to τ_0 yields

$$\begin{aligned} \phi(\tau_0, \tau_1, \tau_2) = - \left(\frac{\kappa_1}{\bar{\omega}_1^2} A_1(\tau_1, \tau_2) + \frac{3}{4} \frac{\sigma}{\bar{\omega}_1^2} A_1^3(\tau_1, \tau_2) \right) \sin \Theta_1 \\ + \frac{1}{36} \frac{\sigma}{\bar{\omega}_1^2} A_1^3(\tau_1, \tau_2) \sin 3\Theta_1 + G(\tau_1, \tau_2) \end{aligned} \quad (16)$$

The secular term in Eq. (16), which appears from a degenerate second-order differential equation and causes a breakdown in the uniformity of the approximation, has been eliminated by the construction of a counter term (see [9]).

The functions A_1 , B_1 , and G that are dependent on the slower time scales can be found from the analysis of the lower-order terms in Eq. (11). It can be shown that A_1 and B_1 are functions of τ_2 only. From the $\mathcal{O}(\epsilon)$ terms of the β equation, by using the approximation $\bar{\omega}_1^2 \approx \omega_1^2 - \frac{3}{4} \lambda A_1^2$ and retaining only terms up to the third order in A_1 , the following amplitude- and phase-correction equations are obtained:

$$\frac{dA_1}{d\tau_2} = \frac{1}{2} \mu A_1 + p_1 A_1^3 \quad \frac{dB_1}{d\tau_2} = p_2 + p_3 A_1^2 \quad (17)$$

where

$$\begin{aligned} \mu &= \eta_1 - \frac{\kappa_1}{\omega_1^2} \eta_2 & p_1 &= -\frac{3}{8} (\eta_2 \sigma + \eta_1 \lambda) \\ p_2 &= -\frac{1}{2} \frac{\kappa_1 \kappa_2}{\omega_1^3} & p_3 &= -\frac{3}{8} \frac{\kappa_2 \sigma}{\omega_1^3} \end{aligned} \quad (18)$$

The solution of the amplitude equation in Eq. (17) is

$$A_1 = \frac{\sqrt{K(\mu/2)} \exp[(\mu/2)\tau_2]}{\sqrt{1 - K p_1 \exp(\mu\tau_2)}} \quad (19)$$

where K is a constant depending on the initial conditions. Equation (19) has the following properties as $t \rightarrow \infty$:

$$A_1 \rightarrow 0 \quad \mu < 0 \quad A_1 \rightarrow \sqrt{-\frac{\mu}{2p_1}} \quad \mu > 0 \quad (20)$$

This solution indicates the presence of a Hopf type of bifurcation in the system with $\mu = 0$ as the bifurcation point. For $\mu < 0$, this particular mode is asymptotically stable. As μ varies from a negative to a positive value, the mode is no longer asymptotically stable. The nature of the bifurcation is determined by the sign of p_1 . If $p_1 > 0$, the bifurcation is of the subcritical type and the mode is divergent. If $p_1 < 0$, a limit-cycle type of oscillation is developed, which is known physically as wing rock.

The homogeneous part of the ϕ solution $[G(\tau_1, \tau_2)]$ can be found by substituting $\phi = G(\tau_1, \tau_2)$ into the $\mathcal{O}(\epsilon)$ terms of the ϕ equation, which leads to

$$G(\tau_1, \tau_2) = A_2(\tau_2) \sin \Theta_2 \quad \Theta_2 \equiv \sqrt{-\kappa_3} \tau_1 + B_2(\tau_2) \quad (21)$$

As can be seen from Eq. (3), the sign of κ_3 is determined by the sign of the yaw damping derivative N_r and the rolling moment derivative due to yaw rate L_r . For most aircraft, these derivatives are negative, and so is κ_3 . Therefore, in most situation this mode is oscillatory. The functions A_2 and B_2 in Eq. (21) can be found from the $\mathcal{O}(\epsilon^3)$ terms of the ϕ equation, which yields

$$\frac{dA_2}{d\tau_2} = \frac{\xi_1}{2} A_2 \quad \frac{dB_2}{d\tau_2} = 0 \quad (22)$$

The solutions of these simple equations are as follows:

$$A_2 = A_{20} \exp\left(\frac{\xi_1}{2} \tau_2\right) \quad B_2 = \text{constant} \quad (23)$$

It is obvious then that the stability of this specific mode is determined by the sign of ξ_1 . This mode is asymptotically stable if $\xi_1 < 0$ and unstable if $\xi_1 > 0$. The value of ξ_1 is affected by the values of the damping derivatives L_p and N_r and the cross-damping derivatives L_r and N_p of the aircraft. At high angles of attack, L_p can be positive. If the other damping derivatives cannot counter the positive L_p to make

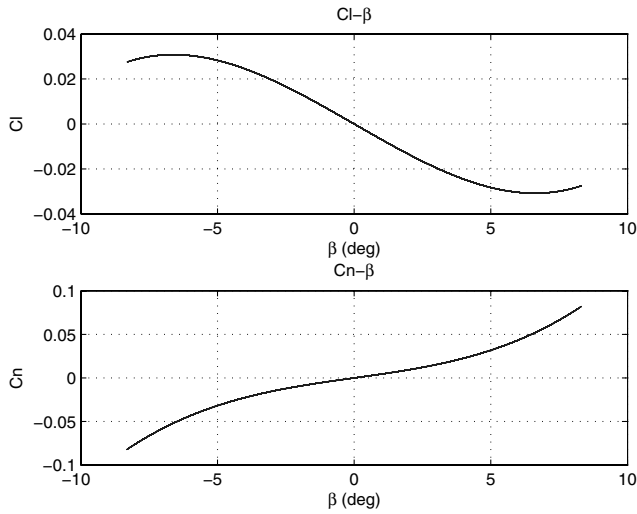


Fig. 3 Static lateral moment nonlinearities used in the simulation.

ξ_1 negative, then this mode is asymptotically unstable and wing rock cannot be sustained in the system.

In the situation in which wing rock occurs ($\mu > 0$, $\xi_1 < 0$, and $p_1 < 0$), its steady-state amplitude is given by the second expression in Eq. (20). The amplitude value depends on p_1 , which is contributed by the nonlinearity coefficients L_{β_1} and N_{β_1} in this case. These results imply that in addition to the satisfaction of $\mu > 0$ and $\xi < 0$, for wing rock to occur, the values of the L_{β_1} and N_{β_1} coefficients must be such

that $p_1 < 0$. In other words, these coefficients have to satisfy the following conditions for wing rock to occur:

$$\eta_2\sigma + \eta_1\lambda > 0 \quad (24)$$

These are the conditions that allow the system to achieve the necessary energy balance to sustain wing rock.

These results confirm the observation in [4] and explain the differences with the analysis carried out in [3]. Further, the results here generalize previous findings by giving explicit conditions for the occurrence of wing rock. Note that the μ expression in Eq. (18) is the same as that obtained in [3], which suggests that this type of nonlinearity does not affect the onset of wing rock.

To examine the accuracy of the results obtained, dynamic response simulations are performed using the aircraft parameters given in the Appendix, subjected to the nonlinearity in the static lateral moments, as shown in Fig. 3, which is associated with $C_{l_{\beta_1}} = 10$ and $C_{n_{\beta_1}} = 15$. In this case, $\mu > 0$, $\xi_1 < 0$, and $\eta_2\sigma + \eta_1\lambda > 0$, which satisfy the wing-rock condition. Figure 4 shows the response of the system to the initial conditions of $\beta(0) = 0.1$ rad and $\phi(0) = 0.05$ rad. As predicted by the analytical results, wing rock does occur in the system. Figure 4 also compares the preceding analytical solution with the numerical integration result. As can be seen, the analytical solution predicts the steady-state amplitude of the wing-rock motion fairly well. A slight phase error in the analytical solution is observed and this error causes the phase shift that becomes obvious after several cycles of oscillations. The transient part of the roll motion is not predicted very accurately by the analytical solution; however, it does show the correct transient trend. This inaccuracy is caused by the error in the homogeneous part of the ϕ solution. Considering the simplicity of the form, however, the analytical solution predicts the overall motion fairly well. Although not shown here, the cases in which the wing-rock conditions are violated are also simulated numerically. Indeed, in such cases, wing rock does not occur in the system and the analytical results predict the stability properties accurately.

V. Conclusions

Lateral-directional aircraft dynamics under cubic variation of lateral moments with respect to sideslip are analyzed in detail. Both weak and strong nonlinearity cases are considered. Using the multiple-time-scales method, approximate solutions are obtained, and from these solutions, stability criterion for each mode of motion as well as the wing-rock occurrence conditions are derived in terms of the moment derivatives. The analytical results are shown to be fairly accurate in predicting the overall motion characteristics.

The results obtained confirm the findings in [3] that the weak static moment nonlinearity does not lead to wing rock. They also confirm the findings in [4], that the static moment nonlinearity can cause wing rock. However, the analysis here shows that wing rock can only occur when the static lateral moment nonlinearities are strong. Moreover, this work shows that the coefficients of the cubic terms have to satisfy a certain condition for the occurrence of wing rock. This condition is mainly affected by the rolling and yawing moment derivatives with respect to roll rate and yaw rate. Such knowledge can be very useful in aircraft design to avoid wing rock or in wing-rock alleviation strategy of an existing aircraft.

Appendix: Generic Fighter Aircraft Parameters for the Simulation

$$\begin{aligned} I_{xx} &= 32,000 \text{ kg} \cdot \text{m}^2 & I_{zz} &= 200,000 \text{ kg} \cdot \text{m}^2 \\ I_{xz} &= 3000 \text{ kg} \cdot \text{m}^2 & b &= 12 \text{ m} & S &= 40 \text{ m}^2 \\ \rho &= 1.225 \text{ kg/m}^3 & \alpha_0 &= 30 \text{ deg} & V &= 100 \text{ m/s} \\ C_l &= -0.4\beta - C_{l_{\beta_1}}\beta^3 - 0.002p - 0.006r + 0.018\dot{\beta} \\ C_n &= 0.25\beta - C_{n_{\beta_1}}\beta^3 - 0.001p - 0.06r - 0.006\dot{\beta} \end{aligned}$$

Note that in the preceding C_l and C_n formulas, the units of the

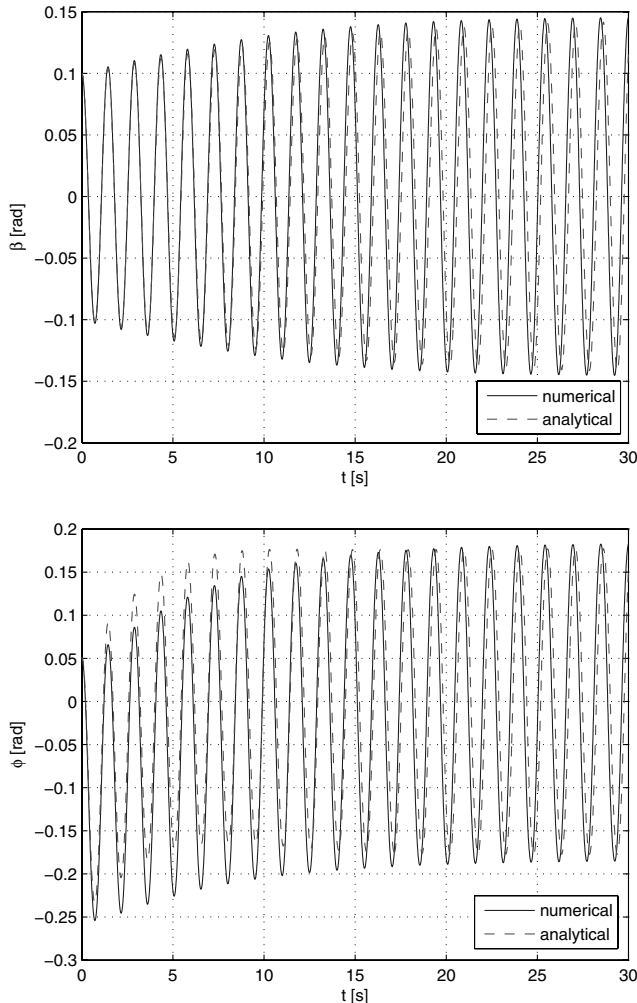


Fig. 4 Responses β and ϕ for $C_{l_{\beta_1}} = 10$ and $C_{n_{\beta_1}} = 15$ with initial conditions $(\beta_0, \phi_0) = (0.1, 0.05)$ rad.

parameters are radian for angle and radian/second for angular rate. For the weak nonlinearity case, $C_{l_{\beta_1}} = 0.1$ and $C_{n_{\beta_1}} = 0.04$. For the strong nonlinearity case, $C_{l_{\beta_1}} = 10$ and $C_{n_{\beta_1}} = 15$.

References

- [1] Go, T. H., and Ramnath, R. V., "An Analytical Approach to the Aircraft Wing Rock Dynamics," AIAA Paper 2001-4426, 2001.
- [2] Go, T. H., and Ramnath, R. V., "Analysis of the Two Degree-of-Freedom Wing Rock in Advanced Aircraft," *Journal of Guidance, Control, and Dynamics*, Vol. 2, No. 2, 2002, pp. 324–333.
- [3] Go, T. H., and Ramnath, R. V., "Analytical Theory of Three Degree-of-Freedom Aircraft Wing Rock," *Journal of Guidance, Control, and Dynamics*, Vol. 27, No. 4, 2004, pp. 657–664.
- [4] Ross, A. J., "Lateral Stability at High Angles-of-Attack, Particularly Wing Rock," *AGARD Conference Proceedings*, CP-260, AGARD, London, 1978, pp. 10.1–10.19.
- [5] Ramnath, R. V. and Sandri, G., "A Generalized Multiple Scales Approach to a Class of Linear Differential Equations," *Journal of Mathematical Analysis and Applications*, Vol. 28, Nov. 1969, pp. 339–364.
doi:10.1016/0022-247X(69)90034-1
- [6] Ramnath, R. V., Hedrick, J. K., and Paynter, H. M. (ed.), *Nonlinear Systems Analysis and Synthesis*, Vol. II, American Society of Mechanical Engineers, New York, 1981, pp. 3–54.
- [7] Byrd, P. F., and Friedman, M. D., *Handbook of Elliptic Integrals for Engineers and Physicists*, Springer-Verlag, New York, 1971.
- [8] Lawden, D. F., *Elliptic Functions and Applications*, Springer-Verlag, New York, 1989.
- [9] Klimas, A., Ramnath, R. V., and Sandri, G., "On the Compatibility Problem for the Uniformization of Asymptotic Expansions," *Journal of Mathematical Analysis and Applications*, Vol. 32, No. 3, 1970, pp. 482–504.
doi:10.1016/0022-247X(70)90272-6
- [10] Chambers, J. R., Grafton, S. B., and Lutze, F. H., "Curved Flow, Rolling Flow, and Oscillatory Pure-Yawing Wind-Tunnel Test Methods for Determination of Dynamic Stability Derivatives," *AGARD Lecture Series*, LS-114, AGARD, London, 1981.